DEVELOPMENTAL DYNAMICS 213:159–169 (1998)

# *Alx-4*, a Transcriptional Activator Whose Expression Is Restricted to Sites of Epithelial–Mesenchymal Interactions

**RHEA HUDSON, AIKO TANIGUCHI-SIDLE, KATA BORAS, O'NEIL WIGGAN, AND PAUL A. HAMEL***
*Department of Laboratory Medicine and Pathobiology, University of Toronto, Toronto, Ontario*

***ABSTRACT*** **We have recently demonstrated that the retinoblastoma family of negative cell cycle regulators can form complexes with a class of developmental factors which contain paired-like (PL) homeodomains (Wiggan et al. [1998] Oncogene 16:227–236). Our screens led to the isolation of a novel PL-homeodomain protein which had been isolated independently by another group and called Alx-4 (Qu et al. [1997] Development 124:3999–4008). Mice homozygous for a targeted null mutation of *Alx-4* have several abnormalities, including preaxial polydactyly, suggesting that *Alx-4* plays a role in pattern formation in limb buds. In data that we present here, we show that *Alx-4* is expressed in mesenchymal condensations of a diverse group of tissues whose development is dependent on epithelial–mesenchymal interactions, many of which are additionally dependent on expression of the HMG-box–containing protein, LEF-1. *Alx-4*–expressing tissues include osteoblast precursors of most bones, the dermal papilla of hair and whisker follicles, the dental papilla of teeth, and a subset of mesenchymal cells in pubescent mammary glands. We show further that Alx-4 strongly activates transcription from a promoter containing the homeodomain binding site, P2. Optimal activation requires specific sequences in the N-terminal portion of Alx-4 as well as a proline-rich region downstream of the PL-homeodomain, but not the paired-tail at the C terminus. Taken together, our results demonstrate that Alx-4 is a potent transcriptional activator that is expressed at sites of epithelial–mesenchymal interactions during murine embryonic development. *Dev. Dyn. 1998;213:159–169.*** 

**Key words: PL-homeodomain protein; epithelial–mesenchymal interactions; LEF-1; murine embryonic development; Alx-4**

## INTRODUCTION

The growth and differentiation of organs and tissues is regulated, in part, by inductive interactions between cells of epithelial and mesenchymal origins (reviewed in Gurdon, 1992). These interactions are reciprocal and sequential, and constitute a chain of signaling events leading to the morphologic development of both tissue layers. The generation of distinct tissues often employs the activities of a common set of developmental factors, supporting the notion that the underlying mechanisms that give rise to different tissues stem from common processes. This paradigm is particularly evident in the development of organs dependent on the invagination of ectodermally-derived epithelial cells into the underlying mesenchyme. Formation of hair and whisker follicles, teeth and mammary glands are prototypes for such processes (for reviews, see (Cunha and Hom, 1996; Hardy, 1992; Thesleff and Nieminen, 1996)).

Recent studies have demonstrated that several classes of factors coordinately mediate the inductive signals between epithelia and mesenchyme in developing limb buds, hair, teeth and/or mammary tissue. These include soluble factors, such as the *B*one *M*orphogenetic *P*roteins (BMPs; for reviews, see Hogan, 1996 a,b) Wnt-family proteins (for reviews, see Cadigan and Nusse, 1996; Kuhl and Wedlich, 1997), as well as transcription factors, such as the homeodomain proteins, Msx1/Msx2 (Chen et al., 1996), and the *H*igh *M*obility *G*roup (HMG) protein, lymphoid enhancer factor-1 (LEF-1) (Travis et al., 1991; van Genderen et al., 1994). Demonstration that the signals from the BMP and Wnt-families of morphogens are integrated by LEF-1 (Kuhl and Wedlich, 1997; Riese et al., 1997) have implied a number of potential downstream targets of these developmental factors, such as the keratin genes in developing hair follicles (Zhou et al., 1995). Indeed, it has been recently proposed that a genetic pathway, which includes Msx1, BMP-4, and LEF-1, induces formation of dental mesenchyme, and that the activities of BMP-4 and Msx1 may reciprocally influence each others' expression in this developing tissue (Chen et al., 1996).

LEF-1 expression is dynamically regulated during embryonic development and is strongly associated with mesenchymal condensations in tissues that arise from the neural crest, such as hair and whisker follicles, teeth, and some skeletal structures, as well as thymus, lung, kidney, brain, mammary glands, and limb buds (Oosterwegel et al., 1993; van Genderen et al., 1994; Zhou et al., 1995). For a subset of these tissues, LEF-1

Grant sponsor: National Cancer Institute of Canada; Grant sponsor: Canadian Cancer Society; Grant sponsor: Medical Research Council of Canada; Grant sponsor: Apotex Inc.; Grant sponsor: Terry Fox Run.
*Correspondence to: Paul A. Hamel, 6318, Medical Sciences Building, 1 King's College Circle, University of Toronto, Toronto, Ontario M5S 1A8, Canada. E-mail: paul.hamel@utoronto.ca
Received 30 March 1998; Accepted 5 June 1998

activity is absolutely required for their development, as demonstrated following generation of mice deficient for LEF-1 (van Genderen et al., 1994). LEF-1 nullizygous mice lack hair, whiskers, teeth, and breast tissue, apparently owing to the failure of mesenchymal condensations adjacent to epithelial cells in the primordia of those tissues to respond to the inductive signals from the epithelial cells. Moreover, forced expression of LEF-1 leads to abnormalities in the positioning and orientation of hair follicles and to ectopic development of teeth (Zhou et al., 1995).

Superimposed on these inductive mechanisms are additional processes that control the proliferation of these same epithelial and mesenchymal cells. Disruption of these cell cycle regulatory pathways also leads to perturbation of normal organogenesis. One class of negative cell cycle regulatory factors is the retinoblastoma (RB) protein family, which includes pRB, p107, and p130 (reviewed in Sidle et al., 1996; Weinberg, 1995). We recently reported that the pRB-family of cell cycle regulatory transcription factors can form complexes with developmental transcription factors that contain paired-like (PL) homeodomains (Wiggan et al., 1998). Our two-hybrid screen of a mouse embryonic day (E) 11 library in these experiments resulted in the isolation of a novel PL-homeodomain protein which was very recently identified independently by Qu et al. (1997) and termed Alx-4. This latter group showed that during early mouse development (E8–E11), *Alx-4* is expressed in mesenchymal cells at distinct sites in the embryo, including the frontonasal mass and the leading edge of limb buds. Mice homozygous for a targeted mutation of *Alx-4* have several abnormalities, including preaxial polydactyly, consistent with a role for *Alx-4* in epithelial–mesenchymal interactions during development of limb buds. *Alx-4* maps very tightly to *Strong's luxoid (lst)* (Qu et al., 1997), which, in addition to the limb defects similar to the *Alx-4* nullizygous mice, exhibit other developmental abnormalities such as dorsal alopecia (Forsthoelfel, 1962).

These other defects suggest that Alx-4 may play a role in the development of other organs dependent on epithelial–mesenchymal interactions. We, therefore, determined the expression pattern of *Alx-4* at later stages of embryogenesis and in specific adult tissues. We show here that *Alx-4* is a potent transcriptional activator and is expressed in specific mesenchymal condensations during the development of hair, whisker, teeth, bone, and breast tissues.

## RESULTS

### Isolation of Alx-4

We screened a murine E11 cDNA library with a GAL4-fusion protein containing the N-terminal portion of p130 (residues 1-415) using the yeast two-hybrid assay (Wiggan et al., 1998). Two of the eight clones isolated encoded proteins which contained PL homeodomains. One of these was identical with MHox (Cserjesi et al., 1992), whereas the second clone encoded a novel PL-homeodomain protein which was recently identified independently and termed Alx-4 (Qu et al., 1997). The isolated full-length cDNA contains an open reading frame of 399 amino acids with a predicted molecular mass of 43 kDa. As expected, Alx-4 is a nuclear factor (Fig. 1). COS cells transfected with influenza hemagglutinin (HA)-tagged full-length Alx-4 ($Alx4^{ATG}$) or the two deletion mutants, $Alx\text{-}4^{NcoI}$ or $Alx\text{-}4^{BamHI}$ (see Fig. 2A), and immunofluorescently labeled with an α-Alx-4 monoclonal antibody reveal the strict nuclear compartmentalization of this protein. Identical localization was observed for these proteins in murine NIH3T3 and human C33A cells (data not shown). Furthermore, a fusion protein between Alx-4 and *G*reen *F*luorescent *P*rotein (GFP) (Cormack et al., 1996; Yang et al., 1996) directed the GFP signal exclusively to the nuclear compartment (K. Boras, unpublished observation).

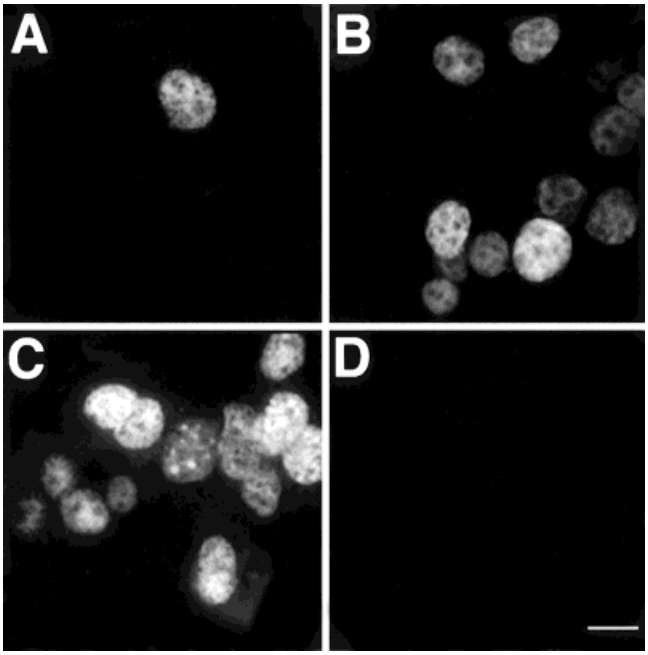


Fig. 1. Nuclear localization of Alx-4 by immunofluorescent labeling. COS cells were transfected with HA-tagged **(A)** $Alx\text{-}4^{ATG}$, **(B)** $Alx\text{-}4^{NcoI}$, or **(C)** $Alx\text{-}4^{BamHI}$ and immunofluorescently labeled with α-Alx-4 monoclonal antibody to demonstrate the strict nuclear localization of Alx-4. Labeling was not detected in **(D)** untransfected COS cells. Bar-5 μm.

We consistently observe that when transcribed and translated in vitro, full-length Alx-4 migrates as two protein products of approximately 49 and 47 kDa (Fig. 2B), these sizes being slightly larger than described previously (Qu et al., 1997). These sizes for Alx-4 are also seen for the endogenous protein, as revealed by western analysis of whole cell lysates from pubescent mouse breast tissue (Fig. 2B, middle lane) and western analysis of whole embryo (E12.5) lysates (data not shown). The second, slightly smaller Alx-4 protein corresponds to an initiation codon at nucleotide 51 (a.a 17) encoding an optimal Kozak consensus sequence (Kozak, 1986). We examined whether ectopic expression of Alx-4 also resulted in two protein products. A

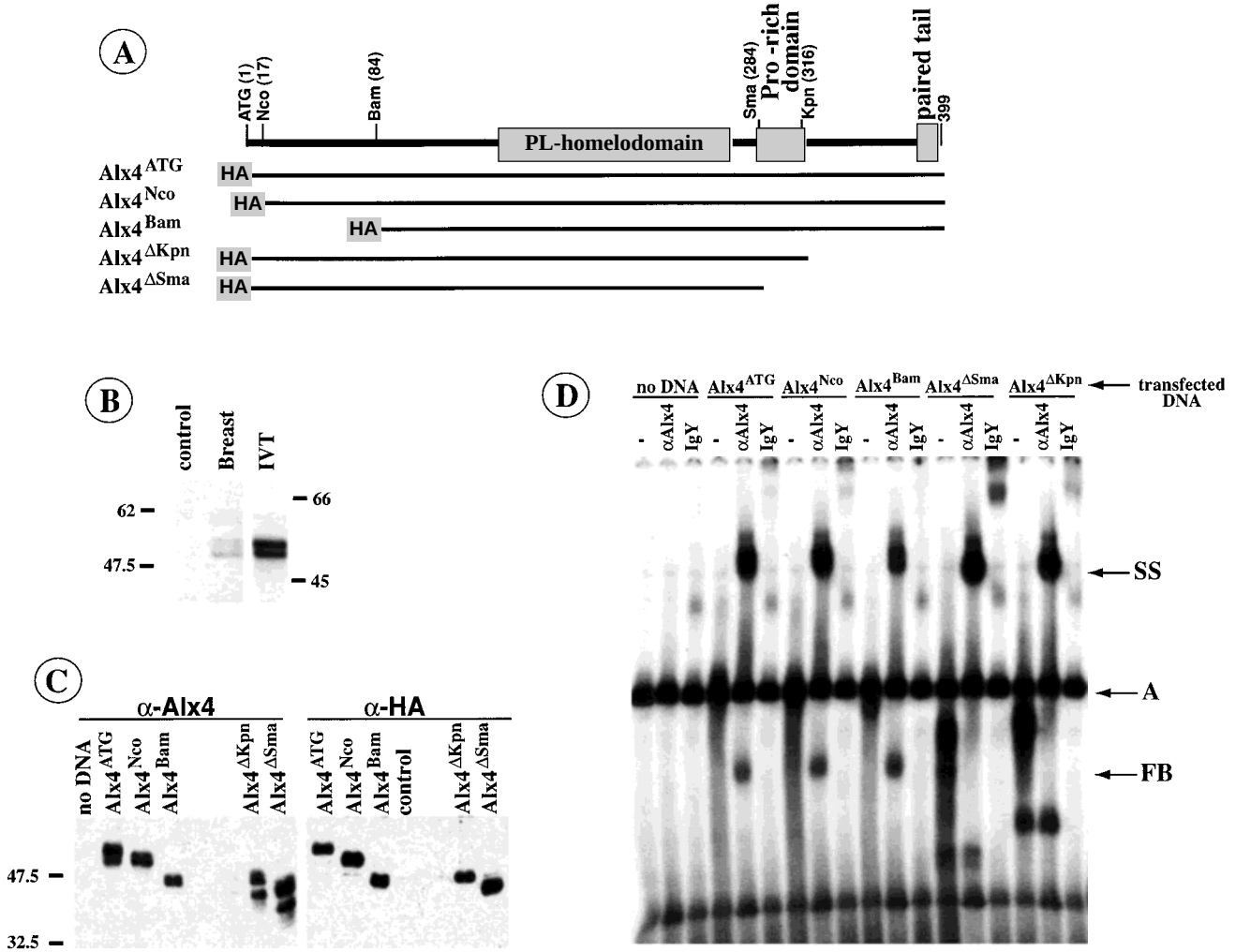


Fig. 2. Specificity of α-Alx-4 monoclonal antibodies and DNA binding activity of Alx-4. **A:** Schematic diagram of the domains within Alx-4 and the corresponding deletion constructs. Numbers represent amino acids. **B:** In vitro transcription and translation (IVT) of Alx-4 produces two polypeptide products of approximately 49 and 47 kDa. Western analysis using α-Alx-4 antibodies shows that endogenously expressed Alx-4 also migrates as two species in total cell lysates (10 µg) of pubescent breast tissue, but not lactating breast tissue (control). **C:** An SV40 expression vector (pECE) encoding a hemagglutinin epitope (HA)-tagged version of full-length Alx-4 (Alx-$4^{ATG}$) and several deletion mutants, Alx-$4^{NcoI}$, Alx-$4^{BamHI}$, Alx-$4^{\Delta KpnI}$, Alx-$4^{\Delta SmaI}$, were transiently transfected into COS cells, and expression was determined by western analysis of nuclear lysates (10 µg) using antibodies directed against Alx-4 (left panel) or the HA epitope (right panel). Specific bands corresponding to the predicted molecular masses of the HA-tagged Alx-4 constructs migrate as doublets or singlets depending on the presence or absence of the second initiation site. Untransfected COS cells (No DNA) or COS cells transfected with irrelevant DNA (control) demonstrate the specificity of the antibodies. **D:** Nuclear lysates (2.0 µg) isolated from untransfected COS cells (No DNA) or COS cells transfected with HA-tagged Alx-$4^{ATG}$, Alx-$4^{NcoI}$, Alx-$4^{BamHI}$, Alx-$4^{\Delta SmaI}$, or Alx-$4^{\Delta KpnI}$ were incubated with a $^{32}$P-labeled oligonucleotide probe encoding the homeodomain-binding site, P2. Supershifts were performed by adding either 40 ng of α-Alx-4 monoclonal antibody or chicken sera directed against the paired-like homeodomain of Alx-4 (IgY) to the reactions before resolving on a 5% non-denaturing polyacrylamide gel. Untransfected COS lysates revealed the presence of an endogenous P2-binding complex, A. The failure to supershift this complex with an α-Alx-4 monoclonal antibody suggests that this complex does not contain Alx-4. COS cells transfected with full-length Alx-4 or Alx-4 mutants show that they all stably bind the P2 sequence. For all mutants, addition of α-Alx-4 antibody produced a strong supershifted band (SS). With the exception of the Alx-$4^{\Delta KpnI}$, a fast migrating band (FB) also appeared.

series of HA-tagged Alx-4 deletion mutants (see Fig. 2A) were transiently expressed in COS cells. Expression was detected by western analysis (Fig. 2C) using either a monoclonal antibody directed against the N-terminal portion of Alx-4 (left panel) or using the α-HA-antibody, 12CA5 (right panel). As is evident in the left panel, whenever the second initiation site was present, two bands for Alx-4 are observed for these ectopically expressed Alx-4 mutants. Use of this second site is most striking in the Alx-$4^{NcoI}$ mutant in which the ATG from the HA tag and the directly fused ATG at the NcoI site are both apparently used. In contrast, we observe only a single band for the expression of Alx-$4^{BamHI}$, this mutant deleting both $Met^{1}$ and $Met^{17}$. That the slower migrating band for each of the mutants initiates from the first Met is verified in the right panel

where only a single band is observed for each of these Alx-4 deletion mutants when the western blots were probed using the α-HA antibody. These bands correspond in molecular weight to the slower migrating bands detected using the α-Alx-4 antibody.

### DNA Binding Activity of Alx-4

We next assessed the DNA-binding activity for each of these Alx-4 deletion mutants in electrophoretic mobility shift assays (EMSA; Fig. 2D). Nuclear lysates from untransfected COS cells or COS cells programmed to transiently express the HA-tagged Alx-4 mutants were incubated with a $^{32}$P-labeled P2 oligonucleotide, which contains a homeodomain-binding site (TAATnnATTA) (Wilson et al., 1995). Untransfected COS lysates reveal the presence of an endogenous P2-binding complex, A. This complex could be competed using unlabeled oligo but was unaffected by competition with an unrelated oligo (data not shown). Complex A does not appear to contain Alx-4 because no alteration of this complex nor the appeareance of a supershifted complex is seen using antibodies specific for Alx-4 (αAlx4 lanes). A relatively weak shift was typically observed, however, when chicken antisera raised against the homeodomain of Alx-4 was employed (IgY lanes), suggesting the presence of another homeodomain protein in the nuclear extracts from these cells. Nuclear lysates from COS cells transfected with each of the Alx-4 mutants demonstrate that all of these mutants are able to stably bind the P2 sequence, as shown by the appearance of supershifted complexes. Alx4$^{ATG}$ and Alx4$^{NcoI}$ run coincidentally with complex A, whereas the Alx4$^{BamHI}$ mutant migrates just slightly faster than the A complex. The deletion mutants, Alx4$^{\Delta SmaI}$ and Alx4$^{\Delta KpnI}$ also bound the P2 oligo. The complexes for these proteins run significantly faster than complex A. For all of these mutants, addition of the α-Alx-4 antibody produced a strong supershifted band (SS) which migrated considerably slower than the unshifted complexes. However, with the exception of the Alx4$^{\Delta KpnI}$, a fast migrating band (FB) also appeared which was specific for cells transfected with these mutants. The nature of this band is unclear.

Because all of these mutant Alx-4 proteins could bind to an oligo encoding a PL-homeodomain binding site (but not a paired domain site; data not shown), we expected that these proteins would affect the activity of a promoter encoding a PL-homeodomain binding site (Fig. 3). Expression plasmids for each mutant were titrated into P19 cells in the presence of a promoter–reporter construct ((P3)$_3$-CAT) containing three tandem copies of a PL-homeodomain binding site, and the relative CAT activity was determined. The full-length version of Alx-4 (Alx4$^{ATG}$) gave the greatest peak activity at 2.5 μg of added DNA. Interestingly, deletion of the first 17 amino acids (Alx4$^{NcoI}$) dramatically reduced the peak level of transactivation. Removal of the first 84 amino acids (Alx4$^{BamHI}$) caused an even further reduction in activity. For both of these latter mutants, addition of up to 10 μg of added plasmid failed to significantly increase activity (data not shown). In contrast to deletions in the N terminus, the last 83 amino acids (Alx4$^{\Delta KpnI}$) had little affect on promoter activity. However, when an additional 32 amino acids were deleted, spanning a relatively proline-rich region, promoter activity reached only 30% of the activity seen for the wild-type protein. Thus, although all of these mutants of Alx-4 are able to bind to DNA, it is clear that sequences both N-terminal and C-terminal to the PL-homeodomain are required for optimal promoter activity.

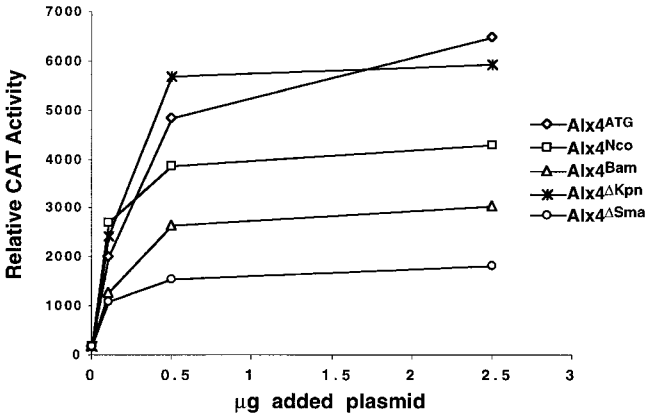


Fig. 3. Full-length Alx-4 is required for optimal activation of transcription from P2-containing promoters. P19 cells were transiently cotransfected by titration of vectors expressing full-length Alx-4 (pcDNA3-CMV-Alx4$^{ATG}$) or truncated versions of Alx-4 (Alx-4$^{NcoI}$, Alx-4$^{BamHI}$, Alx-4$^{\Delta KpnI}$, Alx-4$^{\Delta SmaI}$) and CAT reporter constructs encoding concatemers of a homeodomain binding site ((P3)$_3$-CAT; TAATnnnATTA). Although all versions of Alx-4 are able to bind DNA, it appears that sequences both N-terminal and C-terminal to the PL-homeodomain are required for optimal promotor activity.

### *Alx-4* Is Expressed During Embryogenesis in Cells of Mesenchymal Origin

Because we isolated *Alx-4* from an E11 embryonic mouse library and determined that the levels of its 3.9-kb transcript decreased between E12.5 and E18.5 (data not shown), we determined the tissue specificity of *Alx-4* expression during several stages of embryogenesis using in situ hybridization on whole mouse embryos. Cryosections were hybridized with $^{33}$P-labeled anti-sense RNA probes generated from either the 5′- or 3′-end of *Alx-4* cDNA. The specificity of the hybridization was also confirmed by using sense RNA probes (data not shown).

***Early bone precursors.*** The most striking tissues expressing *Alx-4* at E12.5 are the condensations of mesenchymal cells associated with several different developing organs. The highest levels of expression are observed in regions that eventually give rise to bone (Fig. 4A). These regions include the undifferentiated mesenchymal cells of the primitive ectomeninx (developing cranium), craniofacial bones, and ribs. As was shown previously (Qu et al., 1997), *Alx-4* expression

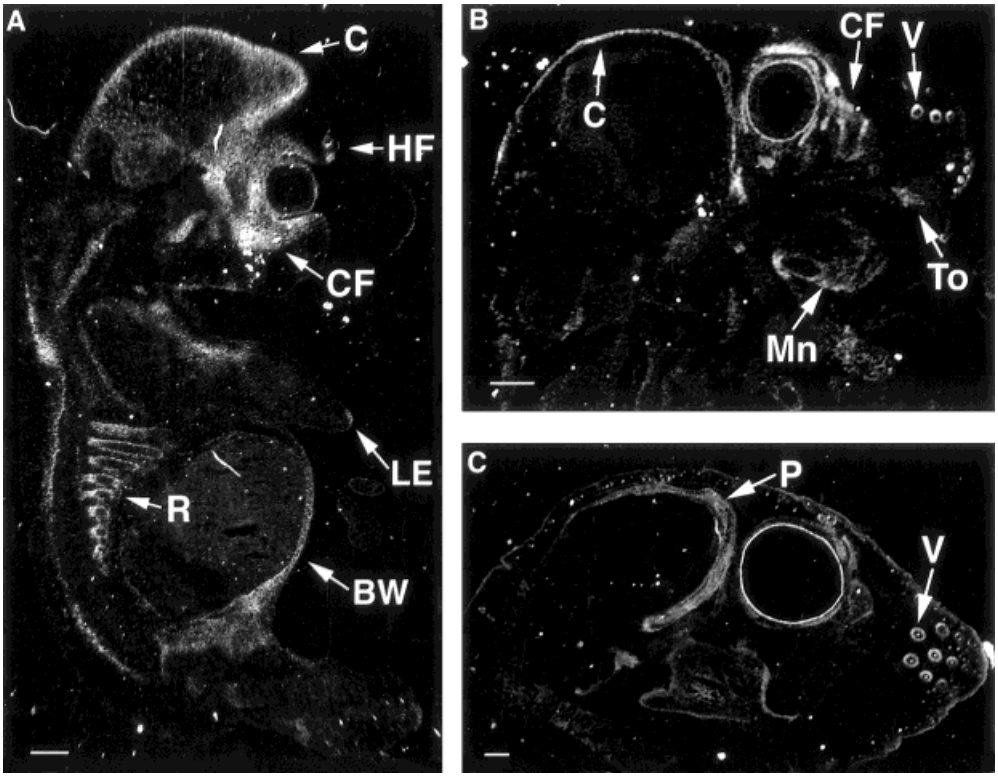


Fig. 4. In situ hybridization of *Alx-4* in sagittal sections of developing embryos. **A:** At E12.5, *Alx-4* is expressed primarily in regions corresponding to the sinus hair follicles (HF), the leading edge (LE) of the developing forelimb, the ventral body wall (BW) and forming skeletal structures including the primitive ectomeninx (developing cranium) (C), craniofacial bones (CF), and ribs (R). **B:** By E15.5, expression of *Alx-4* has become restricted to the craniofacial region where it can be detected in the developing craniofacial bones around the eye and cranium, as well as in the vibrissae (whisker) follicles (V), tooth primordia (To) of the upper right incisor, and developing mandibular bone (Mn). **C:** At E18.5, *Alx-4* expression remains abundant in the vibrissae (V). At this stage, *Alx-4* levels are greatly reduced in the developing craniofacial bones, although low expression is still detected in the maturing parietal (P) bone. Bar-500 μm.

was also detected in the ventral body wall and both the leading edge and anterior aspect of the developing forelimbs.

As embryogenesis progresses to E15.5, some developing bones, such as the ribs, have begun to ossify, whereas in others, the mesenchymal primordia have simply increased in size (Kaufman, 1995). At this stage, high levels of *Alx-4* transcript remain associated with regions of osteogenic potential, particularly in the cranium and craniofacial bones (Fig. 4B). Moderate expression is also observed in the mesenchymal primordia of the mandible outside of Meckel's cartilage. *Alx-4* transcript can not be detected in the ossified ribs at this or any further stages (not shown). It is also evident that *Alx-4* is expressed at very high levels in a tooth primordia of the upper right incisor and in the vibrissae (whisker) follicles.

In the next few days of embryogenesis, the most significant change in the development of bony structures is a substantial increase in the degree of ossification (Kaufman, 1995). By E18.5 (Fig. 4C), expression of *Alx-4* in the developing facial bones has decreased significantly in comparison to E15.5. Only moderate levels of transcript can be detected in the developing parietal and craniofacial bones, demonstrating a significant downregulation of *Alx-4* expression in these bones as they become ossified.

The closely related PL-homeodomain protein Cart-1 (Zhou and Olson, 1994; Zhou et al., 1995) is important in skeletal development, deletion of *Cart-1* giving rise to striking craniofacial defects (Zhao et al., 1996). Given the expression pattern of *Alx-4* in craniofacial bones (Fig. 4) and the ability of PL-homeodomain proteins to heterodimerize, we next determined if *Alx-4* expression was coincident with *Cart-1* expression. Thus, we compared the spatial and temporal expression of *Alx-4* and *Cart-1* (Fig. 5). Serial sections of E15.5 embryos hybridized to *Alx-4* or *Cart-1* demonstrate that these related genes are generally expressed in mutually exclusive regions of developing bony structures, although some areas of overlap are observed. Specifically, *Alx-4*, but not *Cart-1*, is expressed in the ossification centers of the maxilla and nasal bone, the vibrissae follicles, and a discrete cellular layer of the turbinate bones directly adjacent to the nasal epithelium. In contrast, *Cart-1* is exclusively expressed in the thyroid cartilage and turbinate bones. The most significant overlap between *Alx-4* and *Cart-1* expression in the developing embryo at this stage was seen in the ossification centers of the mandible and the frontal bone of the cranium.

***Hair/whisker follicles and teeth.*** Whereas *Alx-4* message levels are strongly reduced between E15.5 and E18.5 in structures giving rise to bone, *Alx-4* transcript is present at high levels in specific mesenchymal condensations giving rise to hair follicles. This expression pattern can first be observed as early as E12.5 when high levels of *Alx-4* transcript are clearly associated with the mesenchymal primordia of the sinus hair follicles (Fig. 4A). As development continues, epithelial cells overlying the mesenchymal condensations invaginate, extend downward, and eventually engulf the mesenchymal cells, thereby forming the dermal papilla.

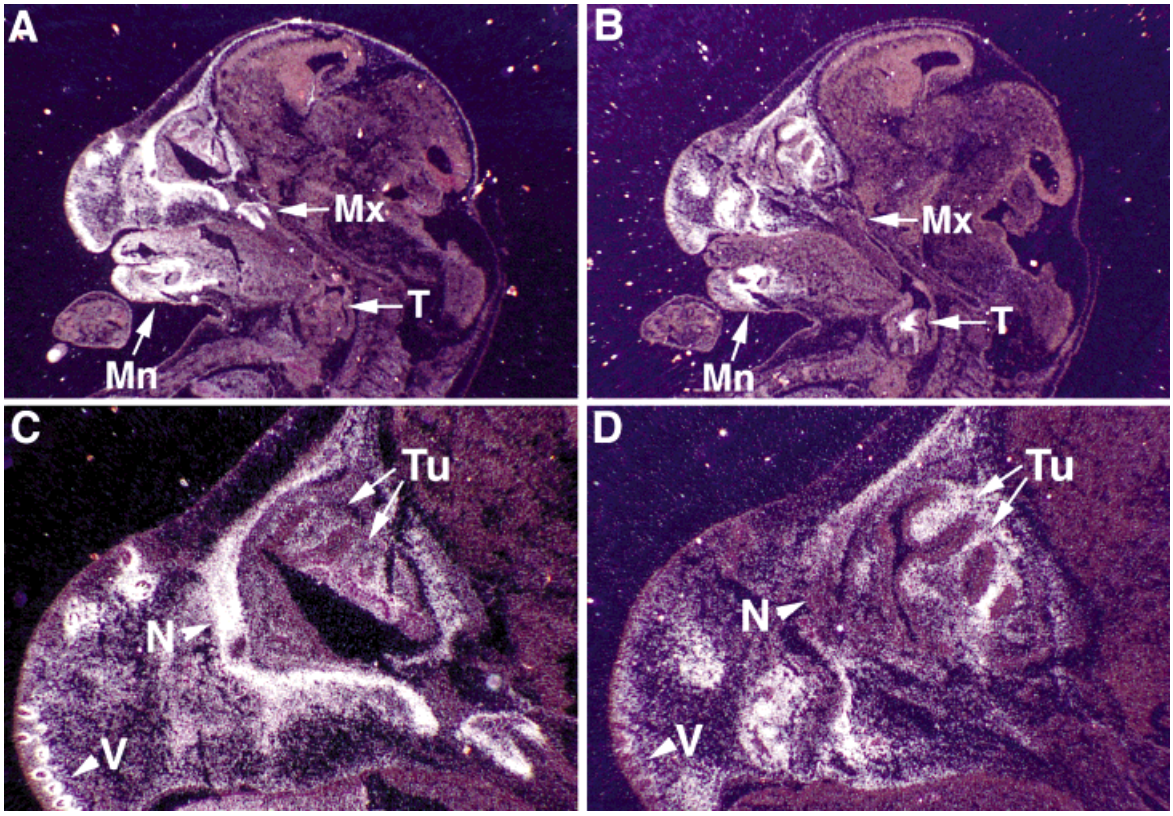


Fig. 5. In situ hybridization of *Alx-4* and *Cart-1* in sagittal sections of E15.5 embryos. Serial sagittal sections were hybridized with riboprobes to *Alx-4* (A, C) or *Cart-1* (B, D). **A:** Strong expression of *Alx-4* is detected in both the developing mandible (Mn) and maxilla (Mx), but not in the thyroid cartilage (T) at this stage. **B:** In contrast, *Cart-1* expression is very abundant in the developing mandible and thyroid cartilage but is undetectable in the maxilla. **C:** Higher magnification of the craniofacial region shows that expression of *Alx-4* is primarily confined to the developing nasal bone (N), vibrissa follicles (V), and a discrete layer of the turbinate bone (Tu) directly adjacent to the nasal epithelium. **D:** In contrast, *Cart-1* transcript is undetectable in the nasal bone and vibrissae follicles, but is strongly expressed throughout the turbinate bones. Bar-500 μm.

At E15.5 and E18.5, high levels of *Alx-4* transcript are detected in the mesenchymal cells of the vibrissae follicles in the facial region (Fig. 4B,C), as well as in developing body hair follicles. As is evident in coronal sections of the nasal region (Figs. 6, 7A,C), *Alx-4* expression is strictly confined to the dermal papilla, the outermost epithelial layer surrounding the dermal papilla, and in all cells of the external root sheath further up the shaft of the whisker. To date, the external root sheath in both whisker and hair follicles is the only example we have found in which *Alx-4* is expressed in cells other than those of mesenchymal origin. Like hair follicles, mesenchymal cells of developing teeth also form a papilla which is engulfed by the invaginating epithelium. It is clear that *Alx-4* is strongly expressed in the dental papillae of the developing incisors but excluded from the dental epithelium (Fig. 6).

### *Alx-4* Expression Overlaps With Expression of *LEF-1*

While apparently not required for bone development, the high mobility group (HMG) protein, LEF-1, is essential for hair/whisker follicle, tooth, and breast development (Kratochwil et al., 1996; van Genderen et

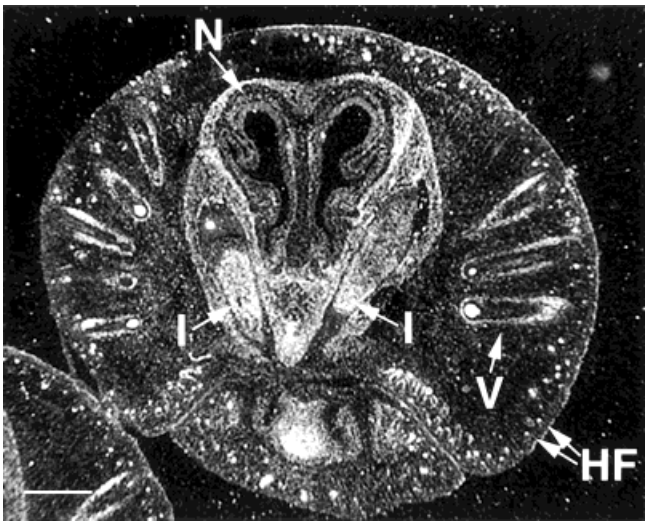


Fig. 6. In situ hybridization of *Alx-4* in coronal sections of E18.5 nasal region. Darkfield image showing expression of *Alx-4* adjacent to the developing nasal bone (N), in the dental papilla of the upper incisors (I), and in the dermal papilla and external root sheath of vibrissae (V) and hair follicles (HF). Bar-500 μm.

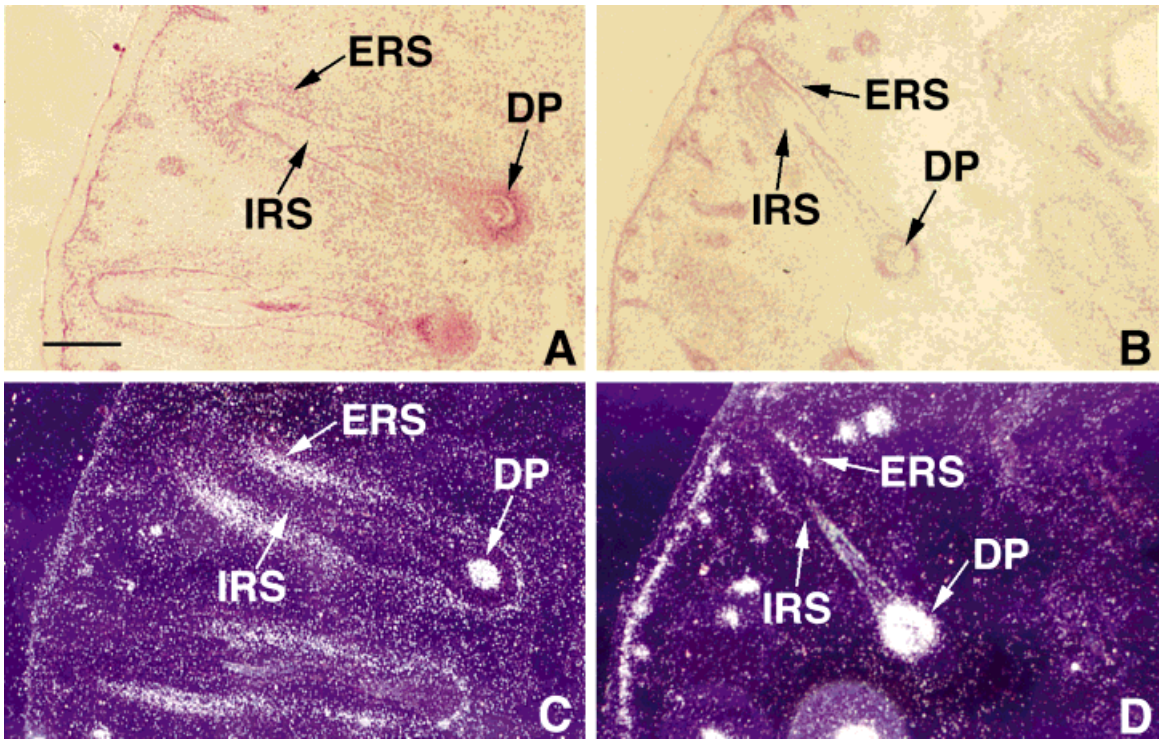


Fig. 7. In situ hybridization of *Alx-4* and *LEF-1* in vibrissa follicles at E18.5. **A** and **C** are brightfield and darkfield images, respectively, demonstrating *Alx-4* expression in the dermal papilla (DP), the outermost layer of epithelial cells surrounding the DP, and external root sheath (ERS) of a single vibrissa follicle. **B** and **D** are brightfield and darkfield images, respectively, showing *LEF-1* expression in the DP, the epithelial cells surrounding the DP, and a single cell layer of the ERS directly adjacent to the internal root sheath (IRS). Bar-200 μm.

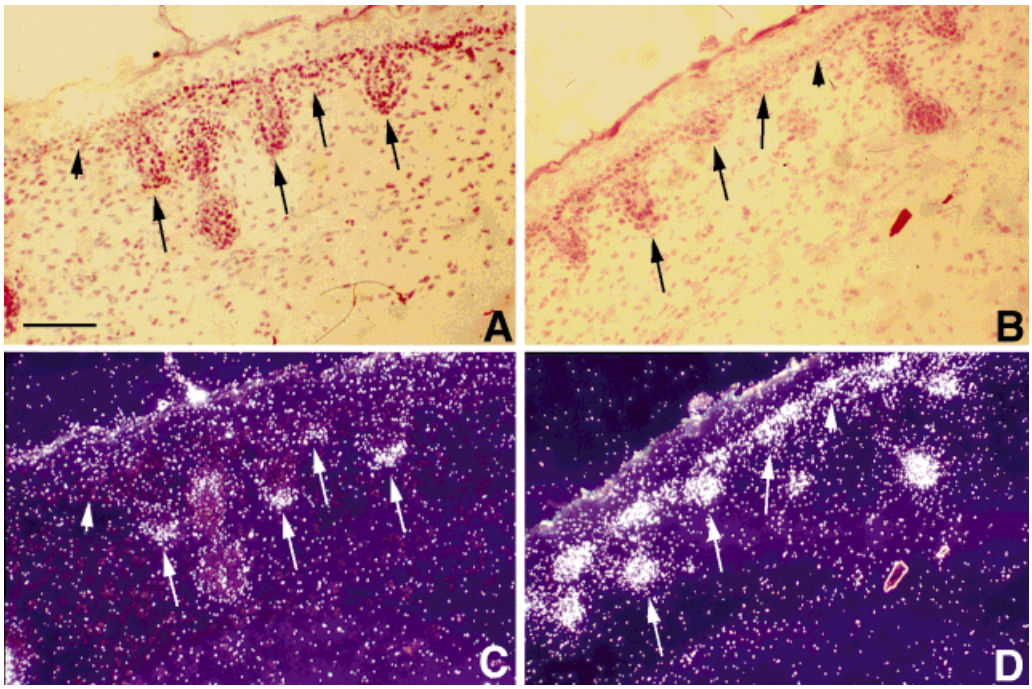


Fig. 8. In situ hybridization of *Alx-4* and *LEF-1* in developing hair follicles. **A** and **C** are brightfield and darkfield images, respectively, showing *Alx-4* expression is confined to the mesenchymal condensations of developing hair follicles (arrows), yet not detectable in the adjacent ectoderm (arrowhead). **B** and **D** are brightfield and darkfield images, respectively, demonstrating that *LEF-1* expression is detected in both mesenchymal condensations (arrows) and in the ectoderm prior to invagination (arrowheads). Bar-100 μm.

al., 1994) by integrating developmental signals leading to mesenchymal condensations (Riese et al., 1997). To begin to understand the relationship between LEF-1 and Alx-4 activity, we examined whether *Alx-4* and *LEF-1* were expressed in overlapping structures by performing in situ analysis on developing vibrissa and body hair follicles of E18.5 embryos. Coronal sections of the nasal region reveal distinct but overlapping expression patterns of *LEF-1* and *Alx-4* (Fig. 7). Like *Alx-4*, *LEF-1* is also expressed in the dermal papilla of the vibrissa follicles as well as all layers of epithelial cells surrounding the dermal papilla. Furthermore, *Alx-4* is expressed in all the cells of the external root sheath, whereas only a single cell layer in the external root sheath directly adjacent to the internal root sheath is strongly positive for *LEF-1* expression.

Given the overlapping expression of *LEF-1* with *Alx-4* in the dermal papilla and the requirement of *LEF-1* in mesenchymal condensations of developing hair/whisker follicles, we wished to determine at what stage of hair development *LEF-1* and *Alx-4* expression were coincident. As Figure 8 illustrates, *Alx-4* expression can only be detected in invaginating hair follicles where significant mesenchymal condensations are observed. In contrast, *LEF-1* is strongly expressed in both the mesenchymal condensations and the adjacent ectodermal cells. Thus, by in situ analysis, *Alx-4* expression in the developing hair follicles occurs only after significant mesenchymal condensations have formed, this latter process being LEF-1 dependent.

***Mammary gland.*** *Alx-4* expression is highly restricted to the dermal and dental papilla of hair/whisker follicles and teeth, respectively. Given that this expression overlaps *LEF-1* expression and that mice deficient in *LEF-1* have no hair, whiskers, teeth, or mammary tissue (van Genderen et al., 1994), which is due apparently to a lack of mesenchymal condensations in these developing tissues, we hypothesized that *Alx-4* would also be expressed in mesenchymal cells in the mammary gland. As Figure 9 demonstrates, *Alx-4* is highly expressed in mesenchymal cells adjacent to the myoepithelial and luminal epithelial cells in breast tissue from pubescent (5 week) female mice. *Alx-4* transcript tends to be restricted to a distinct subpopulation of mesenchymal cells located predominantly near the end buds of the developing ducts.

## DISCUSSION

We and others (Qu et al., 1997) have recently isolated the PL-homeodomain–containing protein, Alx-4, which has striking similarity in its homeodomain and C-terminal region to other PL-homeodomain proteins such as Cart-1 (Zhao et al., 1993), S8 (Kongsuwan et al., 1988), Alx-3 (Rudnick et al., 1994), and Drosophila *aristaless* (Schneitz et al., 1993). Alx-4 strongly activates transcription from a promoter that contains homeodomain-binding sites. Despite all the Alx-4 mutants localizing to the nucleus and being able to bind to DNA encoding a PL-homeodomain consensus sequence, efficient activation requires sequences at the very N-terminal region as well as a proline-rich region in the C terminus, but apparently not the paired-tail motif. Western blot analyses indicate that Alx-4 employs two initiation sites which, by sequencing analysis, are predicted to be separated by 17 amino acids. Although we and others (Qu et al., 1997) have shown that endogenously expressed Alx-4 migrates as a doublet, direct verification of the use of codon 1 and 17 is lacking. Nevertheless, the two protein products harbor dramatically different transactivation abilities as we have demonstrated in Figure 3 where deletion of the first 17 amino acids decreased activated transcription of Alx-4 to approximately 60% of the full-length protein. The biological significance of this observation is currently under investigation.

Some PL-homeodomain proteins, such as Cart-1 (Zhou and Olson, 1994) and goosecoid (Gaunt et al., 1993) and the HMG-box-containing protein, LEF-1 (Zhou et al., 1995), are clearly involved in the inductive pathways of epithelial-mesenchymal signaling during the development of a number of different tissues. Loss of specific members of these families of transcription factors cause deleterious developmental defects in only some of the tissues in which they are expressed (Rivera et al., 1995; van Genderen et al., 1994; Yamada et al., 1995; Zhao et al., 1996), suggestive of a redundancy inherent in the developmental role of these factors in specific tissues. In the very recent report by Qu et al. (1997), loss of Alx-4 produced very specific limb and skeletal defects that are similar to those observed in the mutant mouse strain, *Strong's luxoid (lst)* (Forsthoelfel, 1962). The genetic defect in *lst* mice maps to the *Alx-4* locus. Our in situ analysis of E12.5 to E18.5 embryonic mice predicted that specific defects in the craniofacial structures would be observed as was seen in both the Alx-4 nullizygous and *lst* mice. We also observed very strong expression of *Alx-4* in the dermal papillae of all hair and whisker follicles. While not discussed for the *Alx-4* knock out mouse (Qu et al., 1997), *lst* mice exhibit dorsal alopecia (Forsthoelfel, 1962), consistent with a role for Alx-4 in the generation or maintenance of the dermal papilla in the hair follicles.

Previous studies indicated that *Alx-4* is genetically linked to the signaling pathways generated by the action of the BMPs (Dunn et al., 1997). Our in situ analysis suggests further that *Alx-4* expression may be, in part, under the control of LEF-1 activity or, as we suspect, may cooperate with LEF-1 in generating inductive signals from mesenchymal condensations during bone, breast, and hair/whisker development. Considering the latter tissue, *LEF-1* is initially expressed in discrete foci of the ectoderm, prior to the appearance of mesenchymal condensations. Soon afterward, the presumptive dermal papilla forms subjacent to ectodermal *LEF-1* expression, at which time expression of *LEF-1* is also detected in these mesenchymal condensations

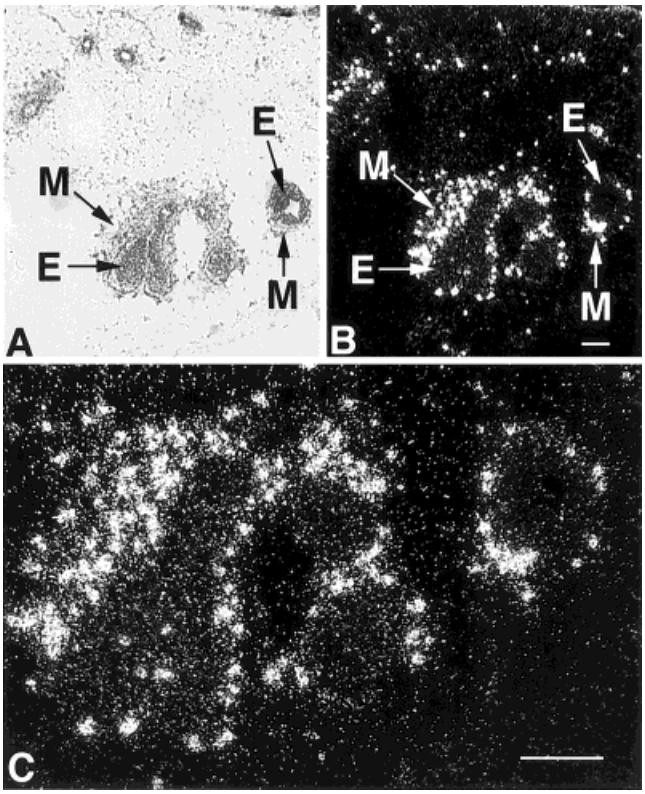


Fig. 9. In situ hybridization of *Alx-4* in pubescent mammary gland. **A:** Brightfield image showing the epithelial (E) composition of the ducts within the mammary gland surrounded by the fibroblast-like mesenchymal cells (M) of the stroma. **B:** Darkfield image of the same field demonstrates that there is strong *Alx-4* expression in the mesenchymal cells directly adjacent to the ducts but that it is undetectable in the myoepithelial and luminal epithelial cells comprising the ducts. **C:** Higher magnification of this area shows that expression is confined to a discrete subpopulation of individual mesenchymal cells. Bar-100 μm.

(Fig. 8). Only when these mesenchymal condensations appear is *Alx-4* detectable. This expression is coincident with the appearance of *LEF-1* in the presumptive dermal papilla. Formation of the dermal papilla in every hair/whisker follicle clearly depends on *LEF-1* expression, because mice deficient for this HMG-box protein have no hair or whiskers (van Genderen et al., 1994). In contrast to *LEF-1,* however, the role for *Alx-4* in hair/whisker development is less obvious. Specifically, whereas *Alx-4* is expressed in the dermal papilla of all hair follicles, alopecia is confined exclusively to the dorsal aspect of *lst* mice. Thus, we hypothesize that Alx-4 may integrate signals important for formation of mature hair/whisker follicles, but only for those follicles on the dorsal aspect of the embryo is *Alx-4* expression absolutely necessary.

*Alx-4* expression in the dermal papilla of hair/whisker follicles predicted its expression in the dental papilla and breast mesenchyme, this prediction being verified in Figures 6 and 9, respectively. However, *lst* mice have apparently normal mammary glands and teeth. We hypothesize that the normal development of these two organs in the *lst* mice is due to their ventral location, and they may, therefore, develop independently of *Alx-4* expression, similar to the ventrally located hair follicles. We suggest further that this dorsal-specific requirement for Alx-4 may occur in the context of LEF-1, supported by data from our laboratory demonstrating that Alx-4 can complex LEF-1 (K. Boras, manuscript in preparation). Overlapping expression of *Alx-4* with the related PL-homeodomain factor, *Cart-1,* may indicate another heterodimeric partner for Alx-4. This notion is supported by craniofacial defects inherent in both Cart-1 (Zhao et al., 1996) and *lst* mice (Forsthoelfel, 1962) and the ability of PL-homeodomain proteins to heterodimerize. Given the many regions of Alx-4 that are presumably involved in protein–protein interactions, including a WW/SH3-binding domain, the PL-homeodomain, a proline-rich region, and the paired-tail motif, we suggest that Alx-4 interacts with a variety of cell-specific factors.

We have shown by in situ hybridization that high levels of *Alx-4* transcript can be detected in a diverse group of organs whose morphogenesis is dependent on epithelial–mesenchymal interactions. The pattern of expression of this PL-homeodomain–containing protein during embryogenesis and that of other PL-homeodomain proteins and LEF-1 suggest that Alx-4 may play a role in modifying the activity of these other developmental factors. Characterization of the pathways that regulate *Alx-4* expression and identification of genes regulated by Alx-4 will provide insight into the role of these inductive interactions during organogenesis.

## EXPERIMENTAL PROCEDURES

### Plasmids, Antibodies, and Yeast Two-Hybrid Screen

$(P3)_3$-CAT reporter constructs were generously provided by J. Epstein (University of Pennsylvania, Philadelphia). Murine *Cart-1* cDNA was kindly provided by Dr. B. de Crombugghe (University of Texas, Houston). Murine *LEF-1* cDNA was kindly provided by Dr. R. Grosschedl (University of California, San Francisco). Monoclonal antibodies against Alx-4 were prepared from mouse splenic B cells after immunization with a His-tagged Alx-4 fusion protein encoding amino acids 85 to 213. A cDNA fragment encoding murine *Alx-4* (residues 156–270) was isolated from a library of murine E11 cDNAs (Clontech, Palo Alto, CA) in a yeast two-hybrid screen using the N-terminal domain of human p130 (residues 1–415) as bait. This fragment was used to isolate a cDNA that encodes full-length *Alx-4* from a λZAP-EXPRESS library of murine embryonic day 15 cDNAs (Stratagene, LaJolla, CA). The sequence of *Alx-4* is identical with that recently reported (Qu et al., 1997).

### Cell Culture and Transfections

Murine P19 embryonal carcinoma cells (McBurney, 1993; Rudnicki and McBurney, 1988) were grown in α-MEM supplemented with 5% fetal calf serum (Sigma,

St. Louis, MO) and 5% bovine donor serum (Cansera, Toronto, Ontario, Canada). Transient transfections of P19 cells were carried out by diluting DNA (plus filler with same promotor) in 100 µL of water and adding 150 µL 0.5 M $CaCl_2$. The DNA solution is added dropwise to 2× Hepes-buffered saline (280 mM NaCl, 50 mM Hepes, 1.5 mM $Na_2HPO_4$), incubated for 30 minutes at room temperature and applied to cells. Plates were placed in the incubator for 10–14 hours before washing 2× in phosphate-buffered saline (PBS) and replacing media. Cells were then harvested 2 days later. Monkey COS kidney cells and mouse NIH 3T3 fibroblasts were grown in Dulbecco's modified Eagle's medium (DMEM) supplemented with 10% fetal calf serum. Transient transfections of COS cells were carried out by washing cells in PBS prior to addition of 0.5 mg/mL diethylaminoethyl (DEAE)-dextran dissolved in 1 M Tris, pH 8. DNA (plus filler with same promotor) was added to the cells and incubated at 37°C for 1 hour, after which the DEAE-dextran solution was replaced with 100 µM chloroquine and further incubated at 37°C for 3 hours. Cells were washed in PBS before replacing with fresh media. Cells were then harvested 2 days later.

### Indirect Immunofluorescence Labeling

COS cells grown on coverslips were rinsed 2× in PBS prior to fixation in cold 100% methanol for 3 minutes. Coverslips were air-dried for approximately 1 hour and stored at −20°C. Cells were immersed in 0.1% bovine serum albumin (BSA)/PBS for 15 minutes to block. Cells were then incubated with monoclonal antibody against Alx-4 diluted in 0.1% BSA/PBS for 30 minutes at room temperature. After thorough washing in 0.1% BSA/PBS, the cells were subsequently incubated in goat anti-mouse immunoglobulin (whole molecule) conjugated to fluorescein isothiocyanate (12.5 µg/ml, Sigma) for 30 minutes at room temperature. The cells were washed several times in 0.1% BSA/PBS and mounted. To image the signal, conventional fluorescence microscopy was carried out with a photomicroscope (Carl Zeiss, Inc. Thornwood, NY) equipped with an epifluorescence attachment.

### In Vitro Translation and Transcription

Full-length mRNA was transcribed using T3 RNA polymerase and pBK-Alx-4, which had been linearized with *Hind III*. $^{35}$S-Labeled Alx-4 was synthesized using rabbit reticulocyte lysate (Promega) and $^{35}$S-methionine (ICN).

### Electrophoretic Mobility Shift Assays (EMSA)

P2 (Wilson et al., 1995) synthetic oligonucleotides were annealed and then end-labeled with $^{32}$P. Next, $4 \times 10^4$ cpm of radiolabeled P2 was incubated with 2.0 µg nuclear lysate in a 21 µL reaction at room temperature for 30 minutes, and the complexes were separated on a 5% non-denaturing acrylamide gel run in 0.25× TBE.

### Promoter Assays

Undifferentiated murine P19 embryonal carcinoma cells were co-transfected with the $(P3)_3$-CAT reporter plasmid, a CMV-β-galactosidase control plasmid, and plasmids encoding murine *Alx-4*, under control of the CMV promotor (pcDNA3). Cells were harvested, lysates were prepared, and CAT and β-galactosidase activities were determined. Relative CAT activity was then calculated by normalization to β-galactosidase activity.

### In Situ Hybridization

Anti-sense and sense radiolabeled RNA probes were generated from fragments of *Alx-4*, *LEF-1*, and *Cart-1* cDNA that had been subcloned into pGEM7 (Promega, Madison, WI). The *Alx-4* anti-sense probe from the 5′-end was a 381-bp *BamHI-PvuII* fragment and was prepared using T7 RNA polymerase. The anti-sense and sense probes from the 3′-end were 550-bp *SmaI-EcoRI* fragments prepared using SP6 or T7 polymerases, respectively. For *LEF-1* anti-sense riboprobes, a 498-bp *XbaI-BamH1* fragment was prepared using SP6 polymerase. For *Cart-1* anti-sense riboprobes, a 296-bp *SacI-SacI* fragment was prepared using SP6 polymerase. In all cases, the radiolabeled nucleotide used was $^{33}$P-UTP (Amersham, Arlington Heights, IL). The probes were used for hybridization at $4 \times 10^4$ cpm/100 µl hybridization buffer.

Whole embryos from pregnant mice or mammary glands from pubescent mice were dissected, quickly frozen in liquid nitrogen-cooled isopentane, and stored at −80°C. Cryosections (6–8 µm) were cut and collected on Superfrost Plus microscope slides (Fisher Scientific, Toronto, Canada), air-dried, and stored at −80°C for no longer than 1 month before use. Slides were fixed for 1 hour in 4% paraformaldehyde/PBS, digested with proteinase K, acetylated with acetic anhydride dissolved in triethanolamine, dehydrated, air-dried, and hybridized overnight at 55°C. High-stringency washing was performed in 50% formamide/2× standard saline citrate (SSC) at 65°C. Subsequent to rinsing in 10 mM Tris pH 8.0, 5 mM NaCl, 5 mM EDTA, slides were treated with ribonuclease A and rinsed sequentially in 2× SSC, 1× SSC, 0.5× SSC at 37°C, followed by 0.1× SSC at 65°C and room temperature. Slides were dehydrated and air-dried before placing under ECL Hyperfilm (Amersham) overnight to determine exposure time in liquid emulsion. Slides were then dipped in equal volumes of Kodak NTB-2 Nuclear Emulsion/0.6M Ammonium Acetate and air-dried. The slides were exposed for 2 to 4 weeks at 4°C, developed in Kodak D-19, and fixed with Kodak Fixer.

## ACKNOWLEDGMENTS

This work was funded by a grant to P.A.H. from the National Cancer Institute of Canada with support from the Canadian Cancer Society as well as an MRC/Industry grant from the Medical Research Council of

Canada and Apotex Inc. A.T.-S. is a research fellow of the National Cancer Institute of Canada with funds provided by the Terry Fox Run.

## REFERENCES


Cadigan KM, Nusse R. Wnt signaling: A common theme in animal development. Genes Dev. 1996;11:3286–3305.

Chen Y, Bei M, Woo I, Satokata I, Maas R. Msx1 controls inductive signaling in mammalian tooth morphogenesis. Development 1996; 122:3035–3044.

Cserjesi P, Lilly B, Bryson L, Wang Y, Sassoon DA, Olson EN. MHox: A mesodermally restricted homeodomain protein that binds an essential site in the muscle creatine kinase enhancer. Development 1992;115:1087–1101.

Cunha GR, Hom YK. Role of mesenchymal-epithelial interactions in mammary gland development. J. Mamm. Gland Biol. Neo. 1996;1: 21–35.

Dunn NR, Winnier GE, Hargett LK, Schrick JJ, Fogo AB, Hogan BLM. Haploinsufficient phenotypes in *BMP4* heterozygous null mice and modification by mutations in *Gli3* and *Alx4*. Dev. Biol. 1997;188:235–247.

Forsthoelfel PF. Genetics and manifold effects of Strong's luxoid gene in the mouse, including its interactions with Green's luxoid and Carter's luxate genes. J. Morphol. 1962;110:391–420.

Gaunt SJ, Blum M, De Robertis E. Expression of the mouse goosecoid gene during mid-embryogenesis may mark mesenchymal cell lineages in the developing head, limbs and body wall. Development 1993;117:769–778.

Gurdon JB. The generation of diversity and pattern in animal development. Cell 1992;68:185–199.

Hardy MH. The secret life of the hair follicle. Trends Genet. 1992;8: 55–61.

Hogan BLM. Bone morphogenetic proteins in development. Curr. Opin. Genet. Dev. 1996a;6:432–438.

Hogan BLM. Bone morphogenic proteins: multifunctional regulators of vertebrate development. Genes Dev. 1996b;10:1580–1594.

Kaufman MH. The Atlas of Mouse Development. San Diego: Academic Press Limited, 1995.

Kongsuwan K, Webb E, Housiaux P, Adams JM. Expression of multiple homeobox genes within diverse mammalian haemopoietic lineages. EMBO J. 1988;7:2131–2138.

Kozak M. Point mutations define a sequence flanking the AUG initiator codon that modulates translation by eukaryotic ribosomes. Cell 1986;44:283–292.

Kratochwil K, Dull M, Farinas I, Galceran J, Grosschedl R. Lef1 expression is activated by BMP-4 and regulates inductive tissue interactions in tooth and hair development. Genes Dev 1996;10: 1382–94.

Kuhl M, Wedlich D. Wnt signalling goes nuclear. Bioessays 1997;19: 101–104.

McBurney MW. P19 embryonal carcinoma cells. Int J Dev Biol 1993;37:135–140.

Oosterwegel M, van de Wetering M, Timmerman J, Kruisbeek A, Destree O, Meijlink F, Clevers H. Differential expression of the HMG box factors TCF-1 and LEF-1 during murine embryogenesis. Development 1993;118:439–48.

Qu S, Niswender KD, Ji Q, van der Meer R, Keeney D, Magnuson MA, Wisdom R. Polydactyly and ectopic ZPA formation in Alx-4 mutant mice. Development 1997;124:3999–4008.

Riese J, Yu X, Munnerlyn A, Eresh S, Hsu S-C, Grosschedl R, Bienz M. LEF-1, a nuclear factor coordinating signaling inputs from *wingless* and *decapentaplegic*. Cell 1997;88:777–787.

Rivera PJ, Mallo M, Gendron MM, Gridley T, Behringer RR. Goosecoid is not an essential component of the mouse gastrula organizer but is required for craniofacial and rib development. Development 1995; 121:3005–3012.

Rudnick A, Ling TY, Odagiri H, Rutter WJ, German MS. Pancreatic beta cells express a diverse set of homeobox genes. Proc. Natl. Acad. Sci. USA 1994;91:12203–12207.

Rudnicki MA, McBurney MW. Cell culture methods and induction of differentiation of embryonyl carcinoma cell lines In: Teratocarcinomas and embryonic stem cells: a practical approach. Robertson, EJ, ed. 1988;19–49.

Schneitz K, Spielmann P, Noll M. Molecular genetics of aristaless, a prd-type homeo box gene involved in the morphogenesis of proximal and distal pattern elements in a subset of appendages in Drosophila. Genes Dev. 1993;7:114–129.

Sidle A, Palaty C, Dirks P, Wiggan O, Kiess M, Gill RM, Wong AK, Hamel PA. Activity of the retinoblastoma-family proteins, pRB, p107 and p130, during cellular proliferation and differentiation. Crit. Rev. Biochem. Mol. Biol. 1996;31:237–271.

Thesleff I, Nieminen P. Tooth morphogenesis and cell differentiation. Curr. Opin. Cell. Biol. 1996;8:844–850.

Travis A, Amsterdam A, Belanger C, Grosschedl R. LEF-1, a gene encoding a lymphoid-specific protein with an HMG domain, regulates T-cell receptor alpha enhancer function. Genes Dev. 1991;5:880–894.

van Genderen C, Okamura RM, Farinas I, Quo RG, Parslow TG, Bruhn L, Grosschedl R. Development of several organs that require inductive epithelial-mesenchymal interactions is impaired in LEF-1-deficient mice. Genes Dev. 1994;8:2691–2703.

Weinberg RA. The retinoblastoma protein and cell cycle control. Cell 1995;81:323–330.

Wiggan O, Taniguchi-Sidle A, Hamel PA. Interaction of the pRB-family proteins with paired-like homeodomains. Oncogene 1998;16: 227–236.

Wilson DS, Guenther B, Desplan C, Kuriyan J. High resolution structure of a paired (Pax) class cooperative homeodimer on DNA. Cell 1995;82:709–719.

Yamada G, Mansouri A, Torres M, Stuart ET, Blum M, Schultz M, De Robertis E, Gruss P. Targeted mutation of the murine goosecoid gene results in craniofacial defects and neonatal death. Development 1995;121:2917–2922.

Yang TT, Cheng L, Kain SR. Optimized codon usage and chromophore mutations provide enhanced sensitivity with the green fluorescent protein. Nuc. Acid. Res. 1996;24:4592–4593.

Zhao GQ, Zhou X, Eberspaecher H, Solursh M, deCrombrugghe B. Cartilage homeoprotein 1, a homeoprotein selectively expressed in chondrocytes. Proc. Natl. Acad. Sci. USA 1993;90:8633–8637.

Zhao Q, Behringer RR, de Crombrugghe B. Prenatal folic acid treatment suppresses acrania and meroanencephaly in mice mutant for the cart-1 homeobox gene. Nature Genetics 1996;13:275–284.

Zhou J, Olsen EN. Dimerization through the helix-loop-helix motif enhances phosphorylation of the transcription activation domains of myogenin. Mol. Cell. Biol. 1994;14:6232–6243.

Zhou P, Byrne C, Jacobs J, Fuchs E. Lymphoid enhancer factor 1 directs hair follicle patterning and epithelial cell fate. Genes Dev. 1995;9:700–713.